AMERICAN SOCIETY FOR MICROBIOLOGY | Journal of Virology®

VACCINES AND ANTIVIRAL AGENTS

Enhancing Neuraminidase Immunogenicity of Influenza A Viruses by Rewiring RNA Packaging Signals

Allen Zheng,[a] Weina Sun,[a] Xiaoli Xiong,[b] Alec W. Freyn,[a] Julia Peukes,[b] Shirin Strohmeier,[a] Raffael Nachbagauer,[a] John A. G. Briggs,[b] Florian Krammer,[a] Peter Palese[a,c]

[a]Department of Microbiology, Icahn School of Medicine at Mount Sinai, New York, New York, USA
[b]Structural Studies Division, Medical Research Council Laboratory of Molecular Biology, Cambridge, United Kingdom
[c]Department of Medicine, Icahn School of Medicine at Mount Sinai, New York, New York, USA

ABSTRACT Humoral immune protection against influenza virus infection is mediated largely by antibodies against hemagglutinin (HA) and neuraminidase (NA), the two major glycoproteins on the virus surface. While influenza virus vaccination efforts have focused mainly on HA, NA-based immunity has been shown to reduce disease severity and provide heterologous protection. Current seasonal vaccines do not elicit strong anti-NA responses—in part due to the immunodominance of the HA protein. Here, we demonstrate that by swapping the 5′ and 3′ terminal packaging signals of the HA and NA genomic segments, which contain the RNA promoters, we are able to rescue influenza viruses that express more NA and less HA. Vaccination with formalin-inactivated "rewired" viruses significantly enhances the anti-NA antibody response compared to vaccination with unmodified viruses. Passive transfer of sera from mice immunized with rewired virus vaccines shows better protection against influenza virus challenge. Our results provide evidence that the immunodominance of HA stems in part from its abundance on the viral surface, and that rewiring viral packaging signals—thereby increasing the NA content on viral particles—is a viable strategy for improving the immunogenicity of NA in an influenza virus vaccine.

IMPORTANCE Influenza virus infections are a major source of morbidity and mortality worldwide. Increasing evidence highlights neuraminidase as a potential vaccination target. This report demonstrates the efficacy of rewiring influenza virus packaging signals for creating vaccines with more neuraminidase content which provide better neuraminidase (NA)-based protection.

KEYWORDS immunodominance, influenza, neuraminidase, packaging signal, vaccine

Influenza virus entry and egress are mediated predominantly by the two major surface glycoproteins, hemagglutinin (HA) and neuraminidase (NA). These two proteins function antagonistically—HA is responsible for sialic acid binding while NA cleaves sialic acid (1). Current seasonal influenza virus vaccination strategies focus heavily on eliciting an immune response against the viral HA, as anti-HA antibodies are often neutralizing and hemagglutination inhibition is an established correlate of protection (2, 3). Antigenic drift of the HA head domain necessitates constant reformulation of seasonal vaccines, and annual vaccine effectiveness is highly variable (4).

Anti-NA antibody titers have been shown to correlate with reductions in both viral shedding and infection severity (3, 5, 6), and small molecules which inhibit NA currently serve as first-line therapeutics for active influenza virus infection (7). The amino acid drift rates for NA are lower than those for HA (8, 9), and substantial evidence exists for the ability of humoral NA antibody responses to confer heterologous protection (10–15).

Despite strong evidence that NA-based immunity is protective, current seasonal

Citation Zheng A, Sun W, Xiong X, Freyn AW, Peukes J, Strohmeier S, Nachbagauer R, Briggs JAG, Krammer F, Palese P. 2020. Enhancing neuraminidase immunogenicity of influenza A viruses by rewiring RNA packaging signals. J Virol 94:e00742-20. https://doi.org/10.1128/JVI.00742-20.

Editor Stacey Schultz-Cherry, St. Jude Children's Research Hospital

Address correspondence to Peter Palese, peter.palese@mssm.edu.

Received 20 April 2020
Accepted 1 June 2020
Accepted manuscript posted online 3 June 2020
Published 30 July 2020

vaccines are only required to contain 15 μg of HA, without standardization of NA content (16). Recent work has demonstrated that, in contrast to natural infection, seasonal vaccination fails to induce robust anti-NA immune responses (17). While a number of platforms such as recombinant NA protein (13–15) or NA-only virus-like particles (VLPs) (18, 19) have been put forth as vaccine candidates, few strategies exist for boosting the host immune response against NA in the context of influenza virus vaccines that also induce HA immunity. HA is the predominant glycoprotein on the virus surface, outnumbering NA at estimates ranging from 4:1 to 14:1 (20, 21), and its immunodominance over NA has been well characterized during both vaccination and infection (22, 23). In this study, we demonstrate that by rewiring the terminal 5′ and 3′ packaging signals of the HA and NA genomic segments, viruses can be rescued that express more NA and less HA. Vaccination with these viruses induces stronger anti-NA humoral responses that protect mice in passive transfer studies against influenza virus challenge.

RESULTS

Design of rewired PR8 virus. Prior studies have demonstrated that segments coding for foreign proteins such as green fluorescent protein (GFP) can be efficiently packaged with the influenza virus genome by flanking the open reading frames (ORFs) of these proteins with variable stretches of nucleotides taken from the 5′ and 3′ termini of influenza virus gene segments (24–30). These terminal stretches, composed of both the untranslated regions (UTRs) and a portion of the ORFs, provide each segment with a unique packaging identity and suggest an explanation for how influenza viruses can efficiently and consistently incorporate their whole genomes into budding virions (31). Previous work from our lab has demonstrated that the packaging signals of two genomic segments can be swapped to rescue rewired viruses that grow to high titers (32).

In this study, the packaging signals of segments 4 and 6, the HA and NA genes, respectively, of A/Puerto Rico/8/1934 (PR8) H1N1 virus were swapped, such that segment 4 was composed of the PR8 H1 ORF flanked by segment 6 packaging signals, and segment 6 was composed of the PR8 N1 ORF flanked by segment 4 packaging signals (Fig. 1A). The nucleotides utilized as segment 6 packaging signals were the 3′ terminal 173 bp and the 5′ terminal 209 bp of the PR8 NA gene segment. The nucleotides utilized as segment 4 packaging signals were the 3′ terminal 99 bp and 5′ terminal 150 bp of the PR8 HA gene segment. The specific nucleotides used as packaging signals were determined based on previous literature (32). Serial synonymous mutations were made to the regions of the termini of the HA and NA ORFs implicated in genome packaging in order to abrogate their residual packaging function. The ATGs located in the coding portions of the introduced packaging signals were mutated to TTGs in order to prevent premature translation of the viral protein. These chimeric segments, termed PR8 NA-HA-NA and PR8 HA-NA-HA, respectively, were used to rescue rewired PR8 virus (PR8-swap) by reverse genetics. Wild-type PR8 virus (PR8-wt) was rescued in parallel (Fig. 1B). PR8-swap virus grew to slightly lower HA titers than PR8-wt virus in embryonated chicken eggs after plaque purification (Fig. 1C).

Since the promoter regions that drive expression of the viral proteins are located in the UTRs of the genomic segments (1), we wanted to assess if rewiring the packaging signals of segments 4 and 6 would alter the abundance of HA and NA on viral particles. Immunoblotting of purified formalin-inactivated PR8-wt and PR8-swap viruses for HA and NA demonstrated clear differences in virion glycoprotein abundance (Fig. 1D). Less HA and more NA were detected in purified PR8-swap virus than in purified PR8-wt virus, suggesting that rewiring the HA and NA packaging signals alters the expression levels of these proteins and their abundance on the viral surface. Purified Newcastle disease virus (NDV) was used as a negative control.

Immunization with rewired PR8 virus induces stronger anti-NA humoral response. Given the altered relative abundance of HA and NA seen in virus with rewired packaging signals, we hypothesized that immunization with PR8-swap virus would elicit

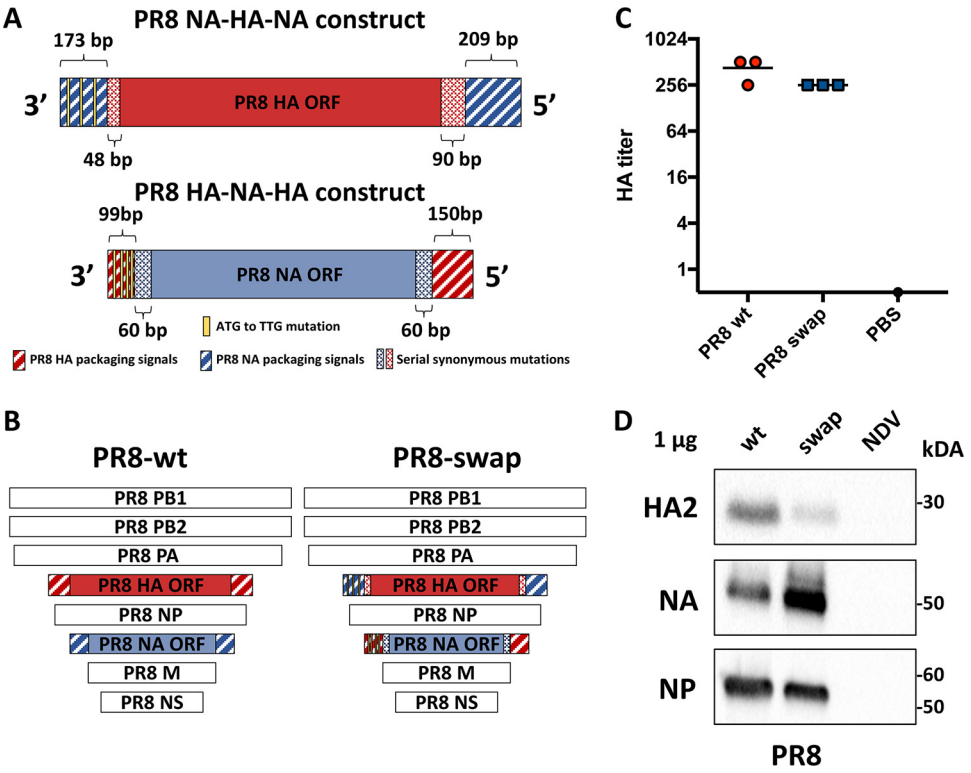

FIG 1 Design and rescue of PR8 virus with swapped HA and NA packaging signals. (A) Design of influenza A virus genomic segments with rewired packaging signals that code for PR8 HA and NA. PR8 NA-HA-NA is composed of the PR8 HA ORF flanked by the 3′ terminal 173 base pairs and the 5′ terminal 209 base pairs of PR8 NA. PR8 HA-NA-HA is composed of the PR8 NA ORF flanked by the 3′ terminal 99 base pairs and the 5′ terminal 150 base pairs of PR8 HA. Serial synonymous mutations were made at the 3′ and 5′ ends of the ORFs in order to abrogate the residual packaging capabilities of these regions. The ATGs (in positive sense) upstream of the HA and NA translation start sites were mutated to TTGs to prevent premature translation. (B) Genomic composition of recombinant viruses containing either wild-type or rewired (swap) PR8 HA and NA segments. (C) Hemagglutination (HA) titers of allantoic fluid containing virus grown in eggs in triplicates. No hemagglutination was observed in PBS control wells. (D) Western blots of proteins from concentrated PR8 wt, PR8 swap, and NDV viruses for influenza virus HA, NA, and NP proteins. One microgram of total protein content from each viral preparation was loaded.

stronger anti-NA and weaker anti-HA antibody responses than immunization with PR8-wt virus. Two groups of 10 6- to 8-week-old BALB/c mice received two 10-μg doses of either formalin-inactivated purified PR8-wt or PR8-swap virus intramuscularly 4 weeks apart. One additional group of mice received two doses of 100 μl phosphate-buffered saline (PBS) as a control. Mice were euthanized 4 weeks after the second dose, and sera were harvested for downstream analysis (Fig. 2A).

Enzyme-linked immunosorbent assays (ELISAs) were performed to determine serum IgG responses against recombinant PR8 H1 and PR8 N1 protein. PR8-swap virus immunization induced a significantly stronger (~1.9-fold) anti-NA IgG response and a significantly weaker (~4.1-fold) anti-HA IgG response than PR8-wt virus immunization. Both vaccination strategies elicited significantly higher antibody titers against HA and NA than the PBS control group (Fig. 2B and C). Pooled sera were used for IgG subtype analysis by ELISA. Swap virus immunization elicited higher IgG1 (~9.7-fold) and IgG2a responses (~1.9-fold) against recombinant PR8 NA protein than wild-type virus immunization (Fig. 2D). High IgG2a titers suggest that these antibodies have undergone more extensive affinity maturation and can better elicit Fc effector functions. These results indicate that, in the context of inactivated influenza virus vaccination, relative abundance is a major determinant of immunogenicity.

Design of clinically relevant H3N2-expressing viruses with rewired packaging signals. The manufacture of inactivated seasonal vaccines typically involves generation of reassortant influenza viruses expressing HAs and NAs of circulating seasonal strains

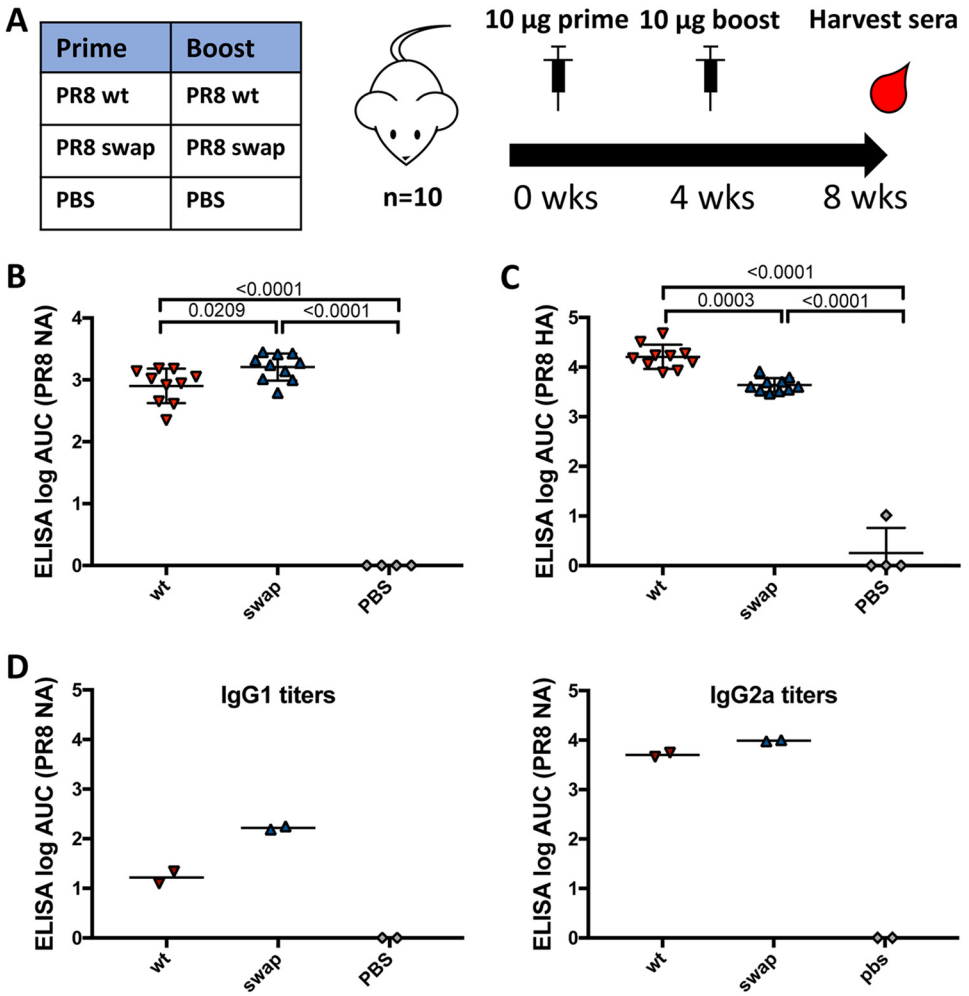

FIG 2 Rewiring HA and NA packaging signals enhances anti-PR8 N1 antibody response in whole-virus vaccination. (A) Mice were vaccinated twice with 10 μg formalin-inactivated purified PR8-wt or PR8-swap virus. Mice were bled 4 weeks postboost, and sera were isolated for downstream analysis. IgG levels to recombinant tetrameric PR8 N1 protein (B) and trimeric PR8 H1 protein (C) were measured by ELISA. (D) Sera from wt- and swap-immunized mice were pooled, and IgG1- and IgG2a-specific ELISAs were performed with recombinant PR8 N1 protein. Log_{10}-transformed area under the curve (AUC) values were compared for all ELISAs. *P* values listed for each comparison were obtained by one-way analysis of variance (ANOVA) with Bonferroni correction.

in a PR8 backbone (33). The H3N2 strain used for the 2016–2017 and 2017–2018 seasonal vaccines was A/Hong Kong/4801/2014 (HK14). To determine if our strategy could be applied to a clinically relevant H3N2-expressing virus, we first designed genomic segments encoding HK14 H3 and N2 with the swapped packaging signals described above (Fig. 3A). PR8 packaging signals were used for optimal incorporation of these segments into the PR8 backbone. Modified HK14 segment 4 (HK14 NA-HA-NA) was composed of the ORF of HK14 H3 flanked by the packaging signals of the PR8 NA gene. Modified HK14 segment 6 (HK14 HA-NA-HA) was composed of the ORF of HK14 N2 flanked by the packaging signals of the PR8 HA gene. ATGs located in the coding portions of the introduced packaging signals were mutated to TTGs in order to prevent premature translation of viral protein as before. These chimeric segments were used to rescue rewired HK14 H3N2-expressing virus (HK14-swap) in a PR8 backbone using reverse genetics. Wild-type HK14 segments 4 and 6 were used to rescue recombinant virus expressing HK14 HA and NA (HK14-wt) in a PR8 backbone, as is consistent with current vaccine design. Similarly to wild-type and rewired PR8 viruses, the HK14-swap virus grew to slightly lower HA titers than HK14-wt virus in embryonated chicken eggs

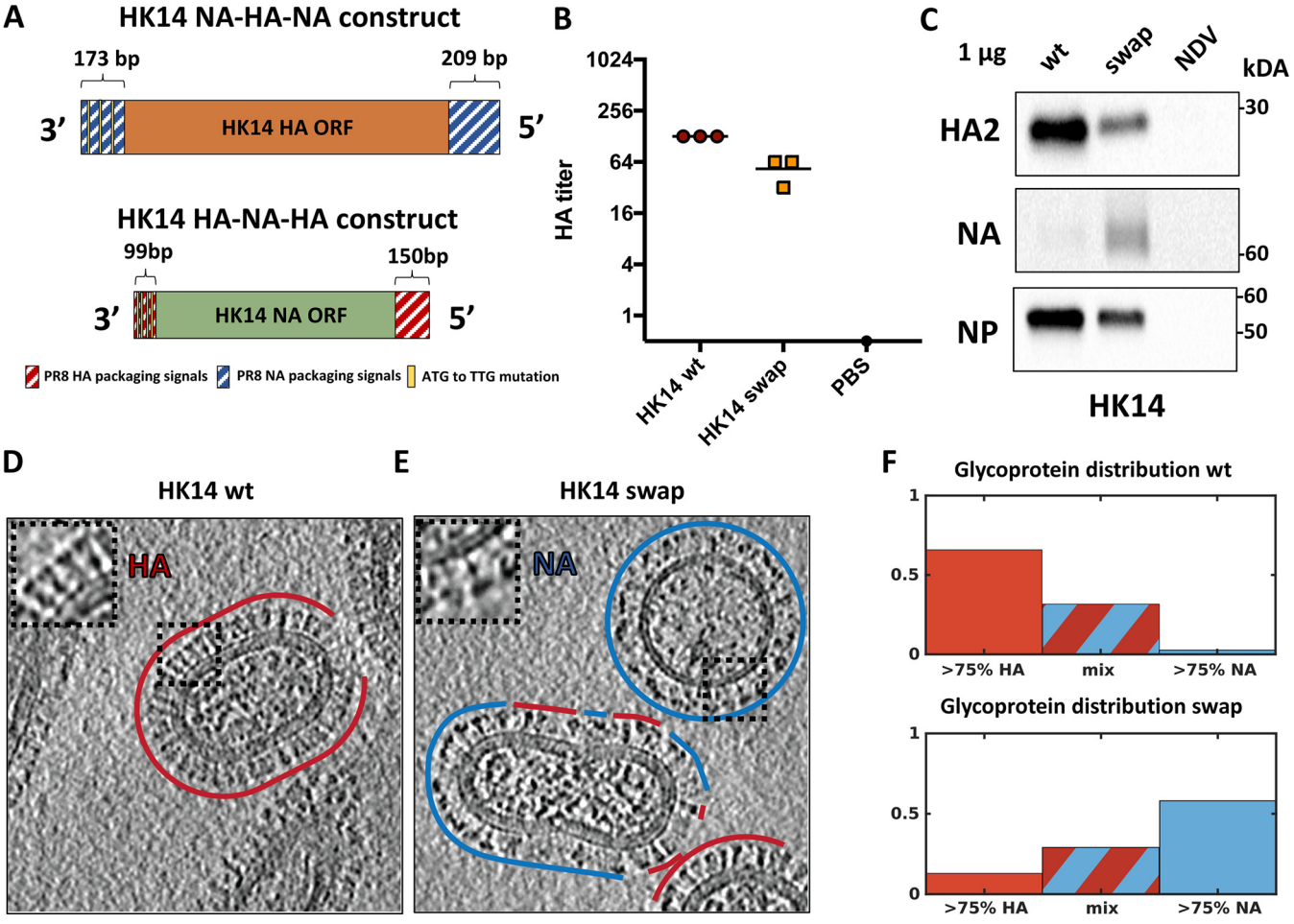

FIG 3 Design and rescue of rewired PR8 virus expressing HK14 HA and NA. (A) Design of influenza A virus genomic segments with rewired packaging signals that code for HK14 HA and NA. HK14 NA-HA-NA is composed of the HK14 HA ORF flanked by the 3′ terminal 173 base pairs and the 5′ terminal 209 base pairs of PR8 NA. HK14 HA-NA-HA is composed of the HK14 NA ORF flanked by the 3′ terminal 99 base pairs and the 5′ terminal 150 base pairs of PR8 HA. The ATGs (in positive sense) upstream of the HA and NA translation start sites were mutated to TTGs to prevent premature translation. (B) Hemagglutination (HA) titers of allantoic fluid containing virus grown in eggs in triplicates. No hemagglutination was observed in PBS control wells. (C) Western blots of proteins from concentrated HK14 wt, HK14 swap, and NDV viruses for influenza virus HA, NA, and NP proteins. One microgram of total protein content from each viral preparation was loaded. (D and E) Computational sections through cryo-electron tomograms of purified viruses show that there are more NA molecules and fewer HA molecules on particles released after infection with HK14 swap virus than with HK14 wt virus. Regions predominantly containing HA glycoproteins are outlined in red. Regions predominantly containing NA glycoproteins are outlined in blue. Magnification shows that the HA has a classic bilobed peanut shape, while the NA has a globular head with a thin stalk. (F) Visual quantification of surface glycoproteins shows that most of the analyzed viral particles in the wild-type sample have >75% HA content, whereas most of the particles in the swap sample have >75% NA content.

and expressed more NA and less HA than HK14-wt virus by immunoblot of formalin-inactivated purified viral particles (Fig. 3B and C).

To confirm the differences observed in HA and NA expression by immunoblot, purified inactivated HK14-wt and HK14-swap viruses were subjected to cryo-electron tomography. Representative tomogram sections show that growth of HK14-swap virus led to the release of particles displaying more NA glycoproteins and fewer HA glycoproteins on their surfaces than HK14-wt virus (Fig. 3D and E). HA molecules are distinguished by their characteristic "peanut" shape, and NA molecules are distinguished by their denser shorter head region (20). To assess the relative abundance of HA and NA on viral particles, quantification of surface glycoproteins was performed on 79 HK14-wt particles and 62 HK14-swap particles. For the majority of analyzed HK14-wt particles, HA comprised more than 75% of observed surface glycoproteins. In contrast, for the majority of analyzed HK14-swap particles, NA comprised more than 75% of observed surface glycoproteins (Fig. 3F).

Immunization with rewired HK14 virus enhances both NA-inhibiting and anti-NA Fc effector function active antibody responses. Next, we sought to compare

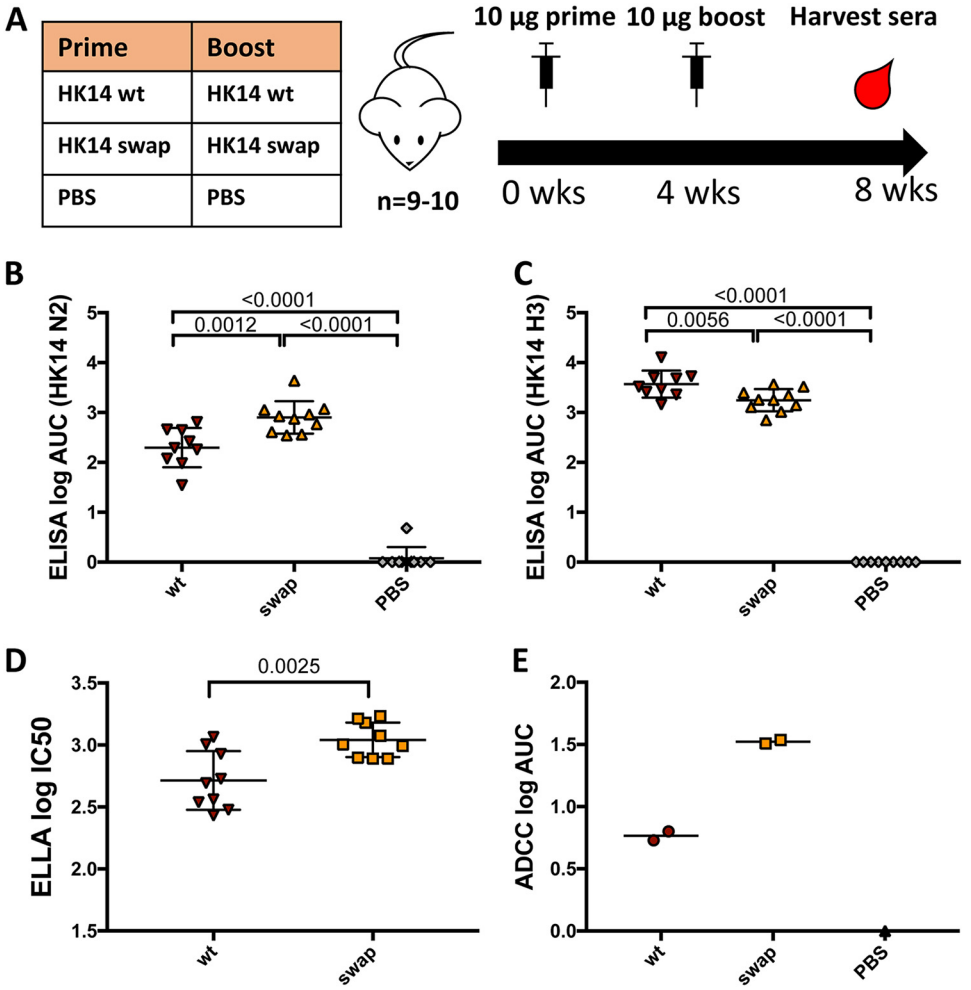

FIG 4 Rewiring HA and NA packaging signals enhances anti-N2 antibody response. (A) Mice were vaccinated twice with 10 μg either formalin-inactivated purified HK14 wt or HK14 swap virus. Mice were bled 4 weeks postboost, and sera were isolated for downstream analysis. IgG levels to recombinant tetrameric HK14 N2 protein (B) and trimeric HK14 H3 protein (C) were measured by ELISA. Log_{10}-transformed area under the curve (AUC) values were compared. (D) Levels of neuraminidase-inhibiting antibodies were measured by ELLA using a recombinant H1N2 virus expressing PR8 H1 and HK14 N2 (H1N2). Log_{10}-reciprocal 50% inhibitory concentration (IC_{50}) values were compared. *P* values listed for all comparisons were obtained by one-way ANOVA with Bonferroni correction. (E) Levels of antibody-dependent cellular cytotoxicity (ADCC)-active antibodies were assessed by ADCC reporter assay performed on MDCK cells infected with H1N2 virus. Sera from each group were pooled and run in duplicates.

the humoral responses elicited by these viruses upon immunization. As before, two groups of 10 6- to 8-week-old BALB/c mice received two 10-μg doses of either formalin-inactivated purified HK14-wt or HK14-swap virus, intramuscularly, 4 weeks apart. A control group of mice received two 100-μl injections of PBS (naive). Mice were euthanized 4 weeks after the second dose, and their sera were isolated for downstream analysis (Fig. 4A).

ELISAs were performed with either recombinant HK14 N2 or HK14 H3 protein to assess IgG responses. Consistent with our data on PR8 viruses, HK14-swap virus immunization induced a significantly stronger (~4-fold) anti-NA IgG response and a significantly weaker (~2.3-fold) anti-HA IgG response than HK14-wt virus immunization. Both immunization regimens elicited significantly higher anti-H3 and anti-N2 responses than PBS (Fig. 4B and C).

We next sought to characterize the functionality of these antibodies in terms of their abilities to inhibit neuraminidase activity and induce Fc receptor-mediated effector functions. A PR8 H1 HK14 N2-expressing virus (H1N2) was used in order to characterize

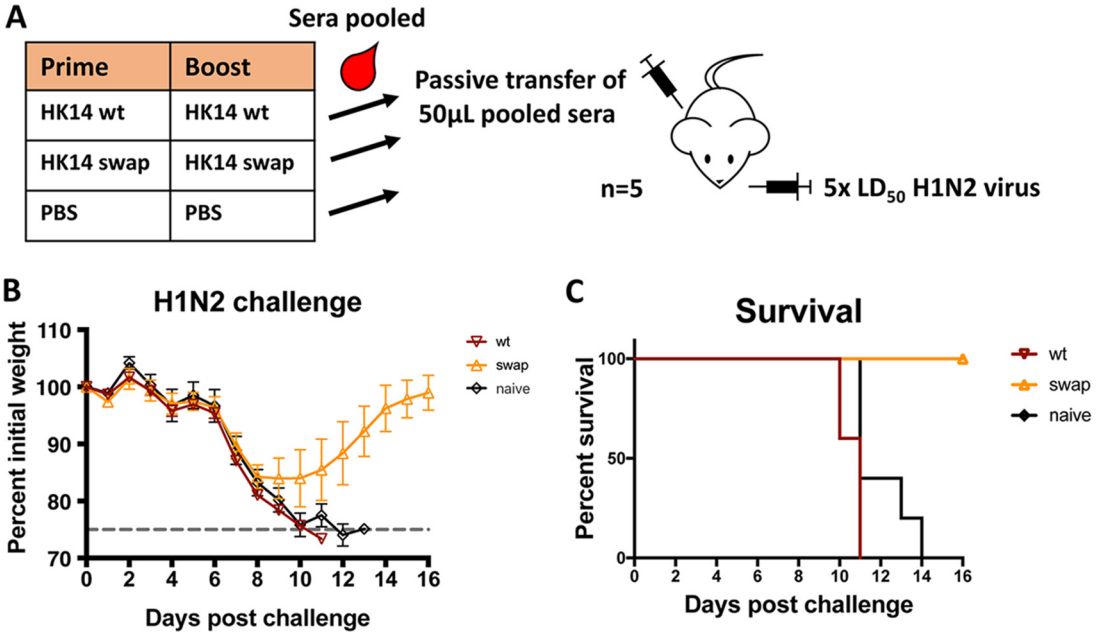

FIG 5 Anti-NA antibody response elicited by swap virus vaccination protects from matched NA influenza virus challenge. (A) Equal amounts of sera isolated from immunized mice were pooled within each group. Pooled sera were passively transferred intraperitoneally to 5 naive mice per group. Two hours posttransfer, mice were infected with five times the median lethal dose (LD_{50}) of a recombinant PR8 virus expressing PR8 HA and HK14 NA. (B and C) Weight loss and survival were measured following infection. Mice that lost >75% of their body weight were euthanized.

the NA-specific humoral response. An enzyme-linked lectin assay (ELLA) was performed using H1N2 virus to assess the capacity of immunized mouse sera to inhibit the enzymatic activity of HK14 N2. Sera raised against HK14-swap virus showed significantly stronger inhibition of N2 activity than sera raised against HK14-wt virus (Fig. 4D).

While inhibition of the viral neuraminidase is the classic mechanism by which anti-NA antibodies are known to function, some antibodies are also able to induce Fc effector functions such as antibody-dependent cellular cytotoxicity (ADCC) (14). We performed an *in vitro* ADCC reporter assay on immunized mouse sera using Madin-Darby canine kidney cells (MDCKs) infected with H1N2 virus. Pooled sera raised against HK14-swap virus showed higher ADCC activity (~5.7-fold) than pooled sera raised against HK14-wt virus (Fig. 4E). These data suggest that our rewired viruses are able to elicit a stronger overall anti-NA humoral response that is better able to both inhibit neuraminidase activity and induce ADCC activity.

Humoral response elicited by rewired virus immunization protects against influenza virus challenge. We next performed passive transfer studies with these sera in order to investigate the protective efficacy of the anti-NA antibody response elicited by the rewired and wild-type HK14 viruses. The same quantity of sera collected from individual immunized mice was pooled for each group. Three groups of five mice received either HK14-wt, HK14-swap, or naive sera by passive transfer. Each mouse was injected intraperitoneally (i.p.) with pooled sera. In order to see the differences in protective efficacy between HK14-wt and HK14-swap sera, only 50 μl of pooled sera was transferred per mouse. Two hours posttransfer, mice were challenged intranasally with five times the median lethal dose (LD_{50}) of an NA-matched H1N2 virus expressing HK14 NA and PR8 HA in order to specifically assess the protection conferred by NA-based immunity (Fig. 5A). Weight loss and survival were measured for 16 days postchallenge. Mice were euthanized upon reaching 75% of their initial body weight. All of the mice that received HK14-swap sera survived, whereas all of the mice that received HK14-wt or naive sera succumbed to the infection (Fig. 5B and C). Thus, immunization with our rewired virus significantly enhances NA-based humoral protection for a clinically relevant NA.

DISCUSSION

Here, we have designed novel chimeric influenza virus genomic segments for which the segment encoding HA has NA packaging signals and the segment encoding NA has HA packaging signals. These constructs can be used to rescue viruses by reverse genetics that express less HA and more NA on the viral surface than viruses with unmodified segments. The effect of this rewiring on the expression of other viral proteins has not been examined.

Consistent with the change in relative abundance of HA and NA, rewired viruses grow to slightly lower but comparable titers. We provide evidence that this change in surface glycoprotein abundance challenges the immunodominance of the HA. By ELISA, there is stronger seroreactivity to purified NA protein and weaker seroreactivity to purified HA protein after immunization with swap virus than with wild-type virus. It is likely that this is due to increased antigenic visibility of the NA in conjunction with decreased antigenic visibility of the HA. This effect is seen for both H1N1- and H3N2-expressing viruses, suggesting a broad applicability for this platform. The stronger NA-specific humoral response is reflected in an increase in both NA-inhibiting (NI)- and ADCC-active antibodies that provide better protection against virus challenge.

Previous work from our lab has demonstrated that extending the NA stalk domain such that the NA protrudes farther than the HA can also increase immunogenicity, suggesting that HA immunodominance is not solely a function of abundance (34). Whether or not package signal rewiring can be combined with stalk extension to further enhance antigenic visibility and immunogenicity of the NA remains to be seen.

While a number of studies have provided evidence that a functional balance between HA and NA abundance is essential for viral fitness (35–37), our data suggest that influenza viruses are viable over a large range of HA-to-NA expression ratios. This is supported by a recent study demonstrating that the relative abundance of viral proteins can vary widely between individual virions (21). It is likely that the functional HA/NA balance is relevant for transmission dynamics, which is unaccounted for when passaging viruses in eggs or tissue culture.

As efforts to improve the breadth and protective efficacy of influenza virus vaccines have redirected focus away from the variable HA head, there has been renewed interest in exploring NA as a target antigen (38, 39). Strategies that are currently being explored include the use of recombinant NA proteins (13–15), virus-like particles (18, 19), and RNA or DNA (12) vaccination approaches. Similar to our work describing extension of the NA stalk as a feasible method for improving NA immunogenicity (34), here we outline a strategy for strengthening NA-based immunity in the context of influenza virus vaccination and demonstrate its protective efficacy in mice. The weaker HA-based humoral response that is elicited can be addressed by supplementation with recombinant HA protein in future vaccine candidates. Importantly, it is unclear if changing the immunogenicity of NA in seasonal vaccines will increase immunological pressure on the NA and thus affect NA drift rates. Our work provides evidence that rewiring HA and NA packaging signals is a viable platform for developing influenza virus vaccines that elicit stronger, more protective NA-based humoral responses.

MATERIALS AND METHODS

Cell culture. Human embryonic kidney 293Ts (HEK 293Ts) were maintained with Dulbecco's modified Eagle's medium (DMEM; Gibco) containing 10% (vol/vol) fetal bovine serum (FBS; HyClone) and 100 U/ml of penicillin-100 μg/ml streptomycin (PS; Gibco). Madin-Darby canine kidney cells (MDCKs) were maintained with minimum essential medium (MEM; Gibco) containing 10% (vol/vol) FBS, 0.15% (w/vol) sodium bicarbonate (Corning), 20 mM HEPES (Gibco), 2 mM L-glutamine (Gibco), and 100 U/ml-100 μg/ml PS. All cells were maintained at 37°C and 5% CO_2.

Rewired segment design, plasmids, and cloning. The rewired segments were designed based on the nucleotide sequences of the HA and NA genes of PR8 H1N1 and HK14 H3N2 viruses (40). Rewired segments were designed with NheI and XhoI restriction enzyme sites flanking the 3′ and 5′ ends, respectively, of the HA and NA ORFs for ease of future cloning. Segments were ordered as synthetic double-stranded DNA fragments (gBlocks; Integrated DNA Technologies) and cloned into an ambisense pDZ vector (41) using the In-Fusion HD cloning kit (Clontech). Products were transformed in DH5α competent cells (Invitrogen), and plasmids were obtained using the QIAprep Spin Miniprep kit (Qiagen). Plasmids were sequence confirmed by Sanger sequencing (Macrogen). The pRS PR8 6-segment plasmid

used here for viral rescue drives ambisense expression of the PR8 PB1, PB2, PA, NP, M, and NS segments. The construction of the pRS PR8 6-segment plasmid employed a similar approach as the construction of the pRS PR8 7-segment plasmid that has been described previously (42).

Rescue of viruses. Viruses were rescued by transfection of HEK 293T cells in six-well plates. HEK 293T cells were transfected with 2.1 μg of PRS PR8 6-segment, 0.7 μg of pDZ HA segment, and 0.7 μg of pDZ NA segment plasmids using TransIT LT1 transfection reagent (Mirus Bio). Transfected cells were cultured at 37°C for 48 h posttransfection, and supernatant was harvested. Eight-day-old embryonated chicken eggs (Charles River) were injected with 200 μl transfection supernatant and incubated at 33°C for 72 h. Eggs were cooled after incubation at 4°C overnight and the allantoic fluids were collected for screening by HA analysis. HA-positive samples were used to plaque-purify virus. Virus was grown on MDCK cells, and the plaques were picked and resuspended in PBS for injection into 10-day-old embryonated eggs. Allantoic fluid was subjected to RNA isolation through a QIAamp Viral RNA minikit (Qiagen). One-step reverse transcription-PCR (RT-PCR) using the Superscript III One-Step-RT-PCR system with Platinum *Taq* DNA polymerase (Invitrogen) was performed on isolated RNA with primers specific to the 5′ and 3′ termini of segments 4 and 6 of PR8 and HK14 (PR8 HA forward, CCGAAGTTGGGGGGGAGCAAAAGCAG GGGAAAATAA; PR8 HA reverse, GGCCGCCGGGTTATTAGTAGAAACAAGGGTGTTTTT; PR8 NA forward, CGAAAGCAGGGGTTTAAAATG; PR8 NA reverse, TTTTTGAACAGACTACTTGTCAATG; HK14 HA forward; GGGAGCAAAAGCAGGGGATAATTC; HK14 HA reverse, GGGTTATTAGTAGAAACAAGGGTGT TTTTAATTA ATG; HK14 NA forward, GGGAGC AAAAGCAGGAGTAAAGATG; HK14 NA reverse, TTATTAGTAGAAACAAG GAGTTTTTTCTAAAATTGCG; Thermo Fisher) to amplify DNA of the genomic segments of interest for sequence confirmation. DNA was isolated by gel purification and sequenced by Sanger sequencing (Genewiz).

Hemagglutination assay. HA assay was performed using 96-well V-bottom plates. Allantoic fluid was serially diluted 2-fold in PBS to a volume of 50 μl/well. A 0.5% suspension of turkey red blood cells (Lampire) in PBS was prepared, and 50 μl was added to each well. Plates were incubated at 4°C and read once red blood cells in the negative control settled to the bottom of the well. HA titer was defined as the highest reciprocal dilution of allantoic fluid that caused agglutination of red blood cells.

Formalin inactivation and purification of viruses. Plaque-purified HA and NA sequence-confirmed influenza viruses were grown in 10-day-old embryonated chicken eggs at 33°C for 72 h. Eggs were refrigerated at 4°C overnight, and allantoic fluids were pooled from 10 to 20 eggs per virus. Pooled allantoic fluid was treated with 0.03% (vol/vol) formalin and incubated at 4°C for 72 h with shaking to inactivate the virus. Inactivation was confirmed by negative plaque assay. Inactivated allantoic fluid was added to 5 ml of 30% (w/vol) sucrose solution in 0.1 M NaCl, 10 mM Tris-HCl, 1 mM EDTA (pH 7.4) in ultracentrifuge tubes (Denville). Samples were spun at 4°C and 25,000 rpm for 2 h with an SW28 rotor in an L7-65 ultracentrifuge (Beckman). Supernatant was aspirated out, and the pellet containing virus was resuspended in 1 ml PBS. Virus was aliquoted and stored at −80°C. Protein concentration of virus preparation was assessed by a Pierce bicinchoninic acid (BCA) protein assay kit (Thermo Fisher).

Immunoblotting. Immunoblotting was performed on formalin-inactivated purified virus. One microgram protein per sample was prepared in Tris-glycine-SDS sample buffer (Invitrogen) and NuPAGE sample reducing agent (Invitrogen) and boiled at 100°C for 5 min before being loaded onto 10% Mini-PROTEAN TGX precast gels (Bio-Rad) and run under denaturing conditions in the presence of sodium dodecyl sulfate (SDS). After running, proteins were transferred onto polyvinylidene difluoride (PVDF) membranes. Color prestained protein standard, broad range (New England BioLabs) was used as a protein size marker. PBS with 5% (wt/vol) fat-free milk powder was used to block membranes for 1 h. Membranes were washed three times with PBS containing 0.05% (vol/vol) Tween 20 (PBS-T). For detection of PR8 proteins, the following antibodies were used: mouse anti-N1 monoclonal antibody 4A5 (43) (1 μg/ml), rabbit anti-H1 (1:3,000, PA5-34929; Thermo Fisher), and rabbit anti-NP (1:3,000, PA5-32242; Invitrogen). For detection of HK14 proteins, the following antibodies were used: mouse anti-H3 monoclonal antibody 12D1 (44) and anti-N2 polyclonal guinea pig sera raised against recombinant N2 protein (generated in-house, 1:2,000). Primary antibodies were diluted in PBS with 1% (w/vol) bovine serum albumin (BSA), and membranes were incubated overnight at 4°C. Membranes were washed three times with PBS-T and incubated with secondary horseradish peroxidase (HRP)-conjugated antibodies (anti-mouse, NXA931V [GE Healthcare]; anti-rabbit, NA9340V [GE Healthcare]; anti-guinea pig, 61-4620 [Invitrogen]) for 1 h at room temperature. All secondary antibodies were diluted 1:3,000 in PBS with 1% (wt/vol) BSA. After washing three times with PBS-T, blots were developed using Pierce ECL Western blotting substrate (Thermo Scientific) and imaged in a ChemiDoc MP imaging system (Bio-Rad).

Cryo-electron tomography. C-Flat 2/2-3C grids were glow discharged for 30 s at 25 mA in a Pelco easiGlow. Solution containing purified virus was diluted with 10-nm colloidal gold, and 2 μl was applied to each grid. Grids were back-side blotted and frozen in liquid ethane using a Leica EM GP2 plunge freezer. Grids were stored in liquid nitrogen until imaging. Imaging was performed on a FEI Titan Krios operated at 300 kV, equipped with a Gatan BioQuantum K3 direct detector using a 20-eV slit width. Tomograms were acquired using SerialEM-3.7.0, collecting between −60° and +60° in a dose-symmetric scheme with a 3° angular increment. The nominal magnification was ×53,000, giving a pixel size of 1.7 Å at the specimen level.

Quantification of amounts of HA and NA in tomograms. Twelve tomograms of HK14-wt virus and 12 tomograms of HK14-swap virus data were pooled into one data set, with the identity of each tomogram blinded to the person doing the analysis. For each virus particle, the distribution of HA and NA on the surface was visually assessed based on the characteristic morphology and symmetry of the proteins. Each particle was assigned to a class: >75% HA, >75% NA, or a mix of HA and NA. A total of

141 virus particles were analyzed: 79 HK14-wt particles and 62 HK14-swap particles. After analysis, the identity of the tomogram was revealed, and the data were presented as histograms.

Mouse immunization and passive transfer studies. Six- to 8-week old female BALB/c mice (Charles River) were immunized intramuscularly with formalin-inactivated purified virus at a dose of 10 μg per mouse after diluting to 100 μl in PBS. Four weeks after the final immunization dose, mice were euthanized and blood was collected by cardiac puncture. Sera were isolated after centrifugation of blood. For passive transfer, equal amounts of sera were taken from each mouse and pooled. Fifty microliters pooled sera was transferred intraperitoneally to 6- to 8-week old female BALB/c mice. Two hours later, mice were anesthetized with a cocktail of ketamine-xylazine and then infected intranasally with five times the LD_{50} of an H1N2 virus expressing PR8 HA and HK14 NA in a PR8 backbone. Weight loss and survival were monitored for 16 days postinfection. All animal experiments were performed in accordance with procedures approved by the Institutional Animal Care and Use Committee of the Icahn School of Medicine at Mount Sinai.

Enzyme-linked immunosorbent assay. ELISAs were used to assess seroreactivity to viral proteins. Area under the curve (AUC) was used as the readout. Purified recombinant trimeric PR8 and HK14 HA and tetrameric PR8 and HK14 NA were produced as described previously (45, 46). Immulon 4 HBX 96-well plates (Thermo Scientific) were coated overnight at 4°C with 2 μg/ml of purified recombinant protein in coating buffer (SeraCare Life Sciences Inc.) at 50 μl per well. The following day, plates were washed three times with 225 μl PBS-T and incubated with 220 μl blocking buffer (3% goat serum, 0.5% nonfat dried milk powder in PBS-T) in each well for 1 h at room temperature (RT). Next, plates were incubated for 2 h at RT with sera that were serially diluted 3-fold in blocking buffer with a starting dilution of 1:50 for NA and 1:100 for HA. The first and last columns were used as plate blanks. Plates were washed with PBS-T three times and incubated with 50 μl/well of anti-mouse IgG horseradish peroxidase (HRP)-conjugated antibody (GE Healthcare), anti-mouse IgG1 HRP-conjugated antibody (Abcam), or anti-mouse IgG2a HRP-conjugated antibody (Abcam) at 1:3,000 dilution in blocking buffer for 1 h. Plates were washed four times with PBS-T before adding 100 μl/well *o*-phenylenediamine dihydrochloride (SigmaFast OPD; Sigma) substrate. The reaction was quenched with 50 μl 3 M HCl after 10 min, and optical density (OD) was measured at 492 nm with a Synergy 4 plate reader (BioTek). The average OD value of the plate blanks plus three standard deviations for each plate was less than 0.07 for all plates. Baseline signal for each plate was set at a value of 0.07 for AUC calculations. AUC was log transformed and graphed using Prism 7.0 (GraphPad). Log_{10} AUC values are reported as means with standard deviations.

Enzyme-linked lectin assay. This assay was performed in accordance with previous reports (47, 48). Immulon 4 HBX 96-well plates (Thermo Scientific) were coated overnight at 4°C with 50 μg per ml of fetuin (Sigma) in coating buffer (SeraCare Life Sciences Inc.). The next day, in a separate 96-well plate, serum samples that had been heat inactivated at 56°C for 30 min were serially diluted 2-fold in PBS starting with a 1:20 dilution and a final volume of 75 μl/well. The first column was left as a virus-only control, and the last column was left for background. H1N2 virus expressing HK14 N2 was diluted in PBS containing 1% BSA to a 90% effective concentration (EC_{90}), and 75 μl/well was added to serially diluted samples and the virus-only control column. The background column received 75 μl/well of PBS with 1% BSA. The plates with serum-virus mixture were incubated at RT for 2 h. One hundred microliters of the serum-virus mixture per well was transferred to the fetuin-coated plates after they had been washed three times with PBS-T. After a 2-h incubation at 37°C, plates were washed three times with PBS-T, and 100 μl/well of peanut agglutinin-horseradish peroxidase conjugate (Sigma) at 5 μg/ml in PBS was added. Plates were incubated in the dark for 1 h before SigmaFast OPD substrate (Sigma) was added. The substrate reaction was quenched with 50 μl 3 M HCl after 10 min, and OD was measured at 492 nm with a Synergy 4 plate reader (BioTek). The values of the averages from the background wells were subtracted from the values of the rest of the plate. The new values were divided by the average of the virus-only wells and multiplied by 100 to get a percentage of NA activity. Percent NI was calculated by subtracting the NA activity from 100%. The 50% inhibitory concentration (IC_{50}) of each serum sample was calculated in Prism 7.0 (GraphPad) by fitting a nonlinear regression. Reciprocal IC_{50} values were log transformed, and statistical significance was assessed by unpaired *t* test, since only two groups were compared.

Antibody-dependent cell-mediated cytotoxicity reporter assay. The capacity of serum antibodies to elicit ADCC was measured using the ADCC Reporter Bioassay kit (Promega Life Sciences). MDCK cells were seeded in a 96-well dish to a total of 2.5×10^4 cells per well in 100 μl complete DMEM with 100 units/ml-100 μg/ml of PS (Gibco) and incubated overnight at 37°C and 5% CO_2. The medium was removed and cells were rinsed with PBS. Cells were then infected with H1N2 virus expressing HK14 NA at a multiplicity of infection of five. Twenty-four hours postinfection, virus was removed from cells, and 25 μl diluted pooled serum was added to each well. Murine ADCC effector cells expressing FcγRIV (Promega) were diluted to add 7.5×10^4 cells per well in RPMI 1640 medium (Gibco) containing 4% Ultra Low IgG FBS (Gibco) in 25 μl. The mixture was allowed to incubate at 37°C and 5% CO_2 for 6 h. After allowing the plate to equilibrate to room temperature, 75 μl of Bio-Glo luciferase (Promega) was added, and luminescence was immediately read on a Synergy 4 plate reader (BioTek). Fold change was calculated as relative luminescence values divided by the average from background wells plus three times the standard deviation. AUC of background-subtracted values was determined using Prism 7.0 (GraphPad), and log_{10} values are reported as means from technical duplicates.

Statistics. All statistical analyses were performed using Prism 7.0 (GraphPad). Statistical differences from all ELISAs were determined using one-way analysis of variance tests with Bonferroni correction for multiple comparisons on log-transformed AUC values. Statistical difference from the ELLA was determined by unpaired *t* test on log-transformed reciprocal IC_{50} values.

ACKNOWLEDGMENTS

We thank Fatima Amanat and Andres Javier for providing recombinant HA and NA proteins. We thank Meagan McMahon for providing anti-N2 guinea pig sera.

Work in the Palese lab was supported by the National Institute of Allergy and Infectious Diseases (NIAID) of the National Institutes of Health under award numbers P01 AI097092, R01AI145870, and F30AI143243. Work in the Briggs laboratory was supported by the Medical Research Council (MC_UP_1201/16) and the European Research Council (ERC) under the European Union's Horizon 2020 research and innovation program (ERC-CoG-648432 MEMBRANEFUSION). Work in the Krammer laboratory was supported by an NIAID Collaborative Influenza Vaccine Innovation Centers (CIVIC) contract (75N93019C00051) and a NIAID Centers of Excellence for Influenza Research and Surveillance (CEIRS) contract (HHSN272201400008C).

A patent application covering the use of viruses with rewired HA and NA packaging signals has been filed under the Icahn School of Medicine at Mount Sinai.

References

1. Shaw ML, Palese P. 2013. *Orthomyxoviridae*, p 1151–1185. *In* Knipe DM, Howley PM (ed), Fields virology, sixth edition. Lippincott Williams & Wilkins, Philadelphia, PA.
2. Wohlbold TJ, Krammer F. 2014. In the shadow of hemagglutinin: a growing interest in influenza viral neuraminidase and its role as a vaccine antigen. Viruses 6:2465–2494. https://doi.org/10.3390/v6062465.
3. Memoli MJ, Shaw PA, Han A, Czajkowski L, Reed S, Athota R, Bristol T, Fargis S, Risos K, Powers JH, Davey RT, Taubenberger JK. 2016. Evaluation of antihemagglutinin and antineuraminidase antibodies as correlates of protection in an influenza A/H1N1 virus healthy human challenge model. mBio 7:e00417-16. https://doi.org/10.1128/mBio.00417-16.
4. Wei C-J, Crank MC, Shiver J, Graham BS, Mascola JR, Nabel GJ. 2020. Next-generation influenza vaccines: opportunities and challenges. Nat Rev Drug Discov 19:239–252. https://doi.org/10.1038/s41573-019-0056-x.
5. Couch RB, Atmar RL, Franco LM, Quarles JM, Wells J, Arden N, Niño D, Belmont JW. 2013. Antibody correlates and predictors of immunity to naturally occurring influenza in humans and the importance of antibody to the neuraminidase. J Infect Dis 207:974–981. https://doi.org/10.1093/infdis/jis935.
6. Monto AS, Petrie JG, Cross RT, Johnson E, Liu M, Zhong W, Levine M, Katz JM, Ohmit SE. 2015. Antibody to influenza virus neuraminidase: an independent correlate of protection. J Infect Dis 212:1191–1199. https://doi.org/10.1093/infdis/jiv195.
7. Johansson BE, Cox M. 2011. Influenza viral neuraminidase: the forgotten antigen. Expert Rev Vaccines 10:1683–1695. https://doi.org/10.1586/erv.11.130.
8. Abed Y, Hardy I, Li Y, Boivin G. 2002. Divergent evolution of hemagglutinin and neuraminidase genes in recent influenza A:H3N2 viruses isolated in Canada. J Med Virol 67:589–595. https://doi.org/10.1002/jmv.10143.
9. Sandbulte MR, Westgeest KB, Gao J, Xu X, Klimov AI, Russell CA, Burke DF, Smith DJ, Fouchier RAM, Eichelberger MC. 2011. Discordant antigenic drift of neuraminidase and hemagglutinin in H1N1 and H3N2 influenza viruses. Proc Natl Acad Sci U S A 108:20748–20753. https://doi.org/10.1073/pnas.1113801108.
10. Chen Z, Kadowaki SE, Hagiwara Y, Yoshikawa T, Matsuo K, Kurata T, Tamura SI. 2000. Cross-protection against a lethal influenza virus infection by DNA vaccine to neuraminidase. Vaccine 18:3214–3222. https://doi.org/10.1016/S0264-410X(00)00149-3.
11. Sylte MJ, Hubby B, Suarez DL. 2007. Influenza neuraminidase antibodies provide partial protection for chickens against high pathogenic avian influenza infection. Vaccine 25:3763–3772. https://doi.org/10.1016/j.vaccine.2007.02.011.
12. Xie H, Li X, Gao J, Lin Z, Jing X, Plant E, Zoueva O, Eichelberger MC, Ye Z. 2011. Revisiting the 1976 "swine flu" vaccine clinical trials: cross-reactive hemagglutinin and neuraminidase antibodies and their role in protection against the 2009 H1N1 pandemic virus in mice. Clin Infect Dis 53:1179–1187. https://doi.org/10.1093/cid/cir693.
13. Wohlbold TJ, Nachbagauer R, Xu H, Tan GS, Hirsh A, Brokstad KA, Cox RJ, Palese P, Krammer F. 2015. Vaccination with adjuvanted recombinant neuraminidase induces broad heterologous, but not heterosubtypic, cross-protection against influenza virus infection in mice. mBio 6:e02556-14. https://doi.org/10.1128/mBio.02556-14.
14. Wohlbold TJ, Podolsky KA, Chromikova V, Kirkpatrick E, Falconieri V, Meade P, Amanat F, Tan J, Tenoever BR, Tan GS, Subramaniam S, Palese P, Krammer F. 2017. Broadly protective murine monoclonal antibodies against influenza B virus target highly conserved neuraminidase epitopes. Nat Microbiol 2:1415–1424. https://doi.org/10.1038/s41564-017-0011-8.
15. McMahon M, Kirkpatrick E, Stadlbauer D, Strohmeier S, Bouvier NM, Krammer F. 2019. Mucosal immunity against neuraminidase prevents influenza B virus transmission in guinea pigs. mBio 10:e00560-19. https://doi.org/10.1128/mBio.00560-19.
16. Air GM. 2012. Influenza neuraminidase. Influenza Other Respir Viruses 6:245–256. https://doi.org/10.1111/j.1750-2659.2011.00304.x.
17. Chen YQ, Wohlbold TJ, Zheng NY, Huang M, Huang Y, Neu KE, Lee J, Wan H, Rojas KT, Kirkpatrick E, Henry C, Palm AKE, Stamper CT, Lan LYL, Topham DJ, Treanor J, Wrammert J, Ahmed R, Eichelberger MC, Georgiou G, Krammer F, Wilson PC. 2018. Influenza infection in humans induces broadly cross-reactive and protective neuraminidase-reactive antibodies. Cell 173:417.e10–429.e10. https://doi.org/10.1016/j.cell.2018.03.030.
18. Easterbrook JD, Schwartzman LM, Gao J, Kash JC, Morens DM, Couzens L, Wan H, Eichelberger MC, Taubenberger JK. 2012. Protection against a lethal H5N1 influenza challenge by intranasal immunization with virus-like particles containing 2009 pandemic H1N1 neuraminidase in mice. Virology 432:39–44. https://doi.org/10.1016/j.virol.2012.06.003.
19. Smith GE, Sun X, Bai Y, Liu YV, Massare MJ, Pearce MB, Belser JA, Maines TR, Creager HM, Glenn GM, Flyer D, Pushko P, Levine MZ, Tumpey TM. 2017. Neuraminidase-based recombinant virus-like particles protect against lethal avian influenza A(H5N1) virus infection in ferrets. Virology 509:90–97. https://doi.org/10.1016/j.virol.2017.06.006.
20. Harris A, Cardone G, Winkler DC, Heymann JB, Brecher M, White JM, Steven AC. 2006. Influenza virus pleiomorphy characterized by cryoelectron tomography. Proc Natl Acad Sci U S A 103:19123–19127. https://doi.org/10.1073/pnas.0607614103.
21. Vahey MD, Fletcher DA. 2019. Low-fidelity assembly of influenza A virus promotes escape from host cells. Cell 176:281.e19–294.e19. https://doi.org/10.1016/j.cell.2018.10.056.
22. Johansson BE, Moran TM, Bona CA, Popple SW, Kilbourne ED. 1987. Immunologic response to influenza virus neuraminidase is influenced by prior experience with the associated viral hemagglutinin. II. Sequential infection of mice simulates human experience. J Immunol 139:2010–2014.
23. Kilbourne ED. 1976. Comparative efficacy of neuraminidase specific and conventional influenza virus vaccines in induction of antibody to neuraminidase in humans. J Infect Dis 134:384–394. https://doi.org/10.1093/infdis/134.4.384.
24. Fujii Y, Goto H, Watanabe T, Yoshida T, Kawaoka Y. 2003. Selective incorporation of influenza virus RNA segments into virions. Proc Natl Acad Sci U S A 100:2002–2007. https://doi.org/10.1073/pnas.0437772100.

25. Muramoto Y, Takada A, Fujii K, Noda T, Iwatsuki-Horimoto K, Watanabe S, Horimoto T, Kida H, Kawaoka Y. 2006. Hierarchy among viral RNA (vRNA) segments in their role in vRNA incorporation into influenza A virions. J Virol 80:2318–2325. https://doi.org/10.1128/JVI.80.5.2318-2325.2006.
26. Marsh GA, Hatami R, Palese P. 2007. Specific residues of the influenza A virus hemagglutinin viral RNA are important for efficient packaging into budding virions. J Virol 81:9727–9736. https://doi.org/10.1128/JVI.01144-07.
27. Goto H, Muramoto Y, Noda T, Kawaoka Y. 2013. The genome-packaging signal of the influenza A virus genome comprises a genome incorporation signal and a genome-bundling signal. J Virol 87:11316–11322. https://doi.org/10.1128/JVI.01301-13.
28. Ozawa M, Maeda J, Iwatsuki-Horimoto K, Watanabe S, Goto H, Horimoto T, Kawaoka Y. 2009. Nucleotide sequence requirements at the 5′ end of the influenza A virus M RNA segment for efficient virus replication. J Virol 83:3384–3388. https://doi.org/10.1128/JVI.02513-08.
29. Ozawa M, Fujii K, Muramoto Y, Yamada S, Yamayoshi S, Takada A, Goto H, Horimoto T, Kawaoka Y. 2007. Contributions of two nuclear localization signals of influenza A virus nucleoprotein to viral replication. J Virol 81:30–41. https://doi.org/10.1128/JVI.01434-06.
30. Liang Y, Hong Y, Parslow TG. 2005. *cis*-Acting packaging signals in the influenza virus PB1, PB2, and PA genomic RNA segments. J Virol 79:10348–10355. https://doi.org/10.1128/JVI.79.16.10348-10355.2005.
31. Hutchinson EC, von Kirchbach JC, Gog JR, Digard P. 2010. Genome packaging in influenza A virus. J Gen Virol 91:313–328. https://doi.org/10.1099/vir.0.017608-0.
32. Gao Q, Palese P. 2009. Rewiring the RNAs of influenza virus to prevent reassortment. Proc Natl Acad Sci U S A 106:15891–15896. https://doi.org/10.1073/pnas.0908897106.
33. Ping J, Lopes TJS, Nidom CA, Ghedin E, MacKen CA, Fitch A, Imai M, Maher EA, Neumann G, Kawaoka Y. 2015. Development of high-yield influenza A virus vaccine viruses. Nat Commun 6:8148. https://doi.org/10.1038/ncomms9148.
34. Broecker F, Zheng A, Suntronwong N, Sun W, Bailey MJ, Krammer F, Palese P. 2019. Extending the stalk enhances immunogenicity of the influenza virus neuraminidase. J Virol 93:e00840-19. https://doi.org/10.1128/JVI.00840-19.
35. Wagner R, Matrosovich M, Klenk HD. 2002. Functional balance between haemagglutinin and neuraminidase in influenza virus infections. Rev Med Virol 12:159–166. https://doi.org/10.1002/rmv.352.
36. Yen H-L, Liang C-H, Wu C-Y, Forrest HL, Ferguson A, Choy K-T, Jones J, Wong DD-Y, Cheung PP-H, Hsu C-H, Li OT, Yuen KM, Chan RWY, Poon LLM, Chan MCW, Nicholls JM, Krauss S, Wong C-H, Guan Y, Webster RG, Webby RJ, Peiris M. 2011. Hemagglutinin-neuraminidase balance confers respiratory-droplet transmissibility of the pandemic H1N1 influenza virus in ferrets. Proc Natl Acad Sci U S A 108:14264–14269. https://doi.org/10.1073/pnas.1111000108.
37. Gaymard A, Le Briand N, Frobert E, Lina B, Escuret V. 2016. Functional balance between neuraminidase and haemagglutinin in influenza viruses. Clin Microbiol Infect 22:975–983. https://doi.org/10.1016/j.cmi.2016.07.007.
38. Krammer F, Fouchier RAM, Eichelberger MC, Webby RJ, Shaw-Saliba K, Wan H, Wilson PC, Compans RW, Skountzou I, Monto AS. 2018. NAction! How can neuraminidase-based immunity contribute to better influenza virus vaccines? mBio 9:e02332-17. https://doi.org/10.1128/mBio.02332-17.
39. Krammer F, Li L, Wilson PC. 2019. Emerging from the shadow of hemagglutinin: neuraminidase is an important target for influenza vaccination. Cell Host Microbe 26:712–713. https://doi.org/10.1016/j.chom.2019.11.006.
40. Broecker F, Liu STH, Sun W, Krammer F, Simon V, Palese P. 2018. Immunodominance of antigenic site B in the hemagglutinin of the current H3N2 influenza virus in humans and mice. J Virol 92:e01100-18. https://doi.org/10.1128/JVI.01100-18.
41. Martínez-Sobrido L, García-Sastre A. 2010. Generation of recombinant influenza virus from plasmid DNA. J Vis Exp 2010:e2057. https://doi.org/10.3791/2057.
42. Fulton BO, Sun W, Heaton NS, Palese P. 2018. The influenza B virus hemagglutinin head domain is less tolerant to transposon mutagenesis than that of the influenza A virus. J Virol 92:e00754-18. https://doi.org/10.1128/JVI.00754-18.
43. Sandbulte MR, Jimenez GS, Boon ACM, Smith LR, Treanor JJ, Webby RJ. 2007. Cross-reactive neuraminidase antibodies afford partial protection against H5N1 in mice and are present in unexposed humans. PLoS Med 4:e59. https://doi.org/10.1371/journal.pmed.0040059.
44. Wang TT, Tan GS, Hai R, Pica N, Petersen E, Moran TM, Palese P. 2010. Broadly protective monoclonal antibodies against H3 influenza viruses following sequential immunization with different hemagglutinins. PLoS Pathog 6:e10007996. https://doi.org/10.1371/journal.ppat.1000796.
45. Margine I, Palese P, Krammer F. 2013. Expression of functional recombinant hemagglutinin and neuraminidase proteins from the novel H7N9 influenza virus using the baculovirus expression system. J Vis Exp 2013:e51112. https://doi.org/10.3791/51112.
46. Krammer F, Margine I, Tan GS, Pica N, Krause JC, Palese P. 2012. A carboxy-terminal trimerization domain stabilizes conformational epitopes on the stalk domain of soluble recombinant hemagglutinin substrates. PLoS One 7:e43603. https://doi.org/10.1371/journal.pone.0043603.
47. Gao J, Couzens L, Eichelberger MC. 2016. Measuring influenza neuraminidase inhibition antibody titers by enzyme-linked lectin assay. J Vis Exp 2016:e54573. https://doi.org/10.3791/54573.
48. Rajendran M, Nachbagauer R, Ermler ME, Bunduc P, Amanat F, Izikson R, Cox M, Palese P, Eichelberger M, Krammer F. 2017. Analysis of anti-influenza virus neuraminidase antibodies in children, adults, and the elderly by ELISA and enzyme inhibition: evidence for original antigenic sin. mBio 8:e02281-16. https://doi.org/10.1128/mBio.02281-16.